Annals of Biomedical Engineering, Vol. 34, No. 3, March 2006 *(© 2006)* pp. 426–435
DOI: 10.1007/s10439-005-9054-8

Development of a Tri-polar Concentric Ring Electrode for Acquiring Accurate Laplacian Body Surface Potentials

W. BESIO, R. AAKULA, K. KOKA, and W. DAI

Department of Biomedical Engineering, Louisiana Tech University, Ruston, LA.

(Received 3 May 2005; accepted 23 September 2005; published online: 16 February 2006)

Abstract—Potentials recorded on the body surface from the heart are of a spatial and temporal function. The 12-lead electrocardiogram (ECG) provides a useful means of global temporal assessment; however, it yields limited spatial information due to the smoothing effect caused by the volume conductor. In an attempt to circumvent the smoothing problem, researchers have used the five-point method (FPM) to numerically estimate the analytical solution of the Laplacian with an array of monopolar electrodes. Researchers have also developed a bipolar concentric ring electrode system to estimate the analytical Laplacian, and others have used a quasi-bipolar electrode configuration. In a search to find an electrode configuration with a close approximation to the analytical Laplacian, development of a tri-polar concentric ring electrode based on the nine-point method (NPM) was conducted. A comparison of the NPM, FPM, and discrete form of the quasi-bipolar configuration was performed over a 400×400 mesh with 1/400 spacing by computer modeling. Different properties of bipolar, quasi-bipolar and tri-polar concentric ring electrodes were evaluated and compared, and verified with tank experiments. One-way analysis of variance (ANOVA) with post hoc *t*-test and Bonferroni corrections were performed to compare the performance of the various methods and electrode configurations. It was found that the tri-polar electrode has significantly improved accuracy and local sensitivity. This paper also discusses the development of an active sensor using the tri-polar electrode configuration. A 1-cm active Laplacian tri-polar sensor based on the NPM was tested and deemed feasible for acquiring Laplacian cardiac surface potentials.

Keywords—ECG, Nine-point method, Quasi-bipolar electrode, Tri-polar electrode, Laplacian, Active sensor.

INTRODUCTION

Body surface potential maps (BSPM) are a method for improving the spatial resolution of electrocardiography (ECG). This can be accomplished by recording from a large number of electrodes on the body surface in contrast to the 12-lead ECG. Since BSPMs utilize surface potentials from disc type electrodes, they also are prone to limited spatial resolution due to the smoothing effect of the volume conductor. The Laplacian, or second spatial derivative of the surface potentials, may assist to sharpen the smoothed potentials. In recent studies by He and Wu[3] and Lian *et al.*[8,9] it was found that body surface Laplacian maps (BSLM) achieved superior spatial resolution in localizing and resolving multiple simultaneously active regional cardiac electrical activities.

Fattorusso and Tilmant[2] were the first investigators to report the use of the concentric ring electrodes in cardiology. Later He and Cohen[4] also used a concentric ring bipolar electrode, which was based on a finite difference numerical approximation method to the analytical solution of the Laplacian operator, the five-point method (FPM). He and Cohen[5] reported that an array of these special bipolar surface Laplacian electrodes had better local sensitivity compared to BSPMs.

This paper will discuss the development of a novel tripolar electrode method for measuring the surface Laplacian electrocardiogram (LECG) that achieves significantly greater accuracy in duplicating the analytical Laplacian, improved spatial resolution, and local sensitivity over concentric bipolar, concentric quasi-bipolar and disc electrode systems. This unique electrode configuration is based upon a finite difference numerical approximation technique, namely the nine-point method (NPM) that is commonly used in image processing for edge detection purposes. Computer models were designed to verify the accuracy and local sensitivity capability of concentric electrode systems. These computer models were verified using tank experiments followed by the design of a one-centimeter diameter active Laplacian tri-polar sensor based on the NPM to verify that human LECG signals could be acquired with this sensor.

BACKGROUND THEORY

Five-Point Method (FPM)

In Fig. 1, v_0 through v_{12} are the corresponding potentials for points p_0 through p_{12}. The Laplacian, Δ at point p_0 due to the potentials v_5, v_6, v_7, v_8, and v_0 with spacing of $2r$, which forms the five-point arrangement, can be obtained using the Taylor series expansion and finite difference approximation

Address correspondence to W. Besio, 711 South Vienna St, Ruston, LA 71270. Electronic mail: walterb@latech.edu

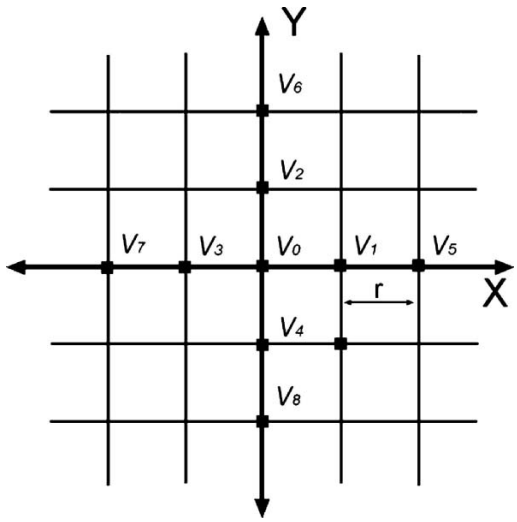

FIGURE 1. Arrangement of the FPM and NPM on a regular plane square grid of size $N \times N$ and spacing $r = 1/N$. v_0 through v_{12} are the potentials at points p_0 through p_{12}, respectively. v_5, v_6, v_7, v_8, and v_0 form the FPM and v_0 through v_8 forming the NPM.

methods as explained by Ames[12] and results in (1)

$$\left(\frac{\partial^2 v}{\partial x^2} + \frac{\partial^2 v}{\partial y^2}\right)\Big|_{p_0} = \Delta p_0 = \frac{1}{(2r)^2}\left(\sum_{i=5}^{8} v_i - 4v_0\right) + O((2r)^2) \quad (1)$$

where $O((2r)^2) = \frac{(2r)^2}{4!}\left(\frac{\partial^4 v}{\partial x^4} + \frac{\partial^4 v}{\partial y^4}\right)\Big|_{p_0} + \frac{(2r)^4}{4!}\left(\frac{\partial^6 v}{\partial x^6} + \frac{\partial^6 v}{\partial y^6}\right)\Big|_{P_0} + \cdots$ is truncation error.

The approximation to the Laplacian of potential at p_0 is then

$$\Delta p_0 \cong \frac{4}{(2r)^2}(\bar{v} - v_0) \quad (2)$$

where $\bar{v} = \frac{1}{4}\sum_{i=5}^{8} v_i$ is the average of the potentials of the four points.

According to Husikamp[6], the discrete Equation (2) can be applied to a disc and concentric ring bipolar electrode system by performing the integral along the circle of radius $2r$ around the point p_0 of the Taylor expansion and defining $X = 2r\cos(\theta)$ and $Y = 2r\sin(\theta)$, as shown in (3).

$$\Delta p_0 \cong \frac{4}{(2r)^2}\frac{1}{2\pi}\int_0^{2\pi} (v(2r,\theta) - v_0)\, d\theta \quad (3)$$

This approach shows how the FPM is an approximation to the bipolar concentric ring electrode.

Quasi-Bipolar Method (QBM)

The QBM uses points p_1 to p_8 and p_0 as seen in Fig. 1. The QBM was analyzed in discrete fashion using the finite difference method for comparison with the FPM and NPM in approximating the Laplacian. The potentials at p_5 to p_8 and p_0 were averaged together as if they are shorted. This difference method was generalized for the quasi-bipolar electrode configuration to verify the quasi-bipolar Laplacian estimate, which is shown in Appendix. The Laplacian at p_0 is given as

$$\Delta p_0 = \left(\frac{\partial^2 v}{\partial x^2} + \frac{\partial^2 v}{\partial y^2}\right)\Big|_{p_0} = \frac{4}{r^2}\left[\frac{1}{2}\left(\frac{1}{4}\sum_{i=5}^{8} v_i + v_0\right) - \frac{1}{4}\sum_{j=1}^{4} v_j\right] + O(r^2) \quad (4)$$

where

$O(r^2) = \frac{2}{r^2}\left[O(r^4)\right] = \frac{7r^2}{48}\left(\frac{\partial^4 v}{\partial x^4} + \frac{\partial^4 v}{\partial v^4}\right)\Big|_{p_0} + \cdots$, is the truncation error.

This can be generalized to quasi-bipolar concentric ring electrode as (5)

$$\Delta v_0 \cong \frac{4}{r^2}\left(\frac{\frac{1}{2\pi}\int_0^{2\pi}(v(2r,\theta) + v_0)d\theta}{2} - \frac{1}{2\pi}\int_0^{2\pi} v(r,\theta)\, d\theta\right) \quad (5)$$

where $\frac{1}{2\pi}\int_0^{2\pi} v(r,\theta)\, d\theta$ and $\frac{1}{2\pi}\int_0^{2\pi} v(2r,\theta)\, d\theta$ represent the average potentials on the middle ring and outer ring, respectively.

In the quasi-bipolar configuration, the electrode has three elements (a disc, middle ring and an outer ring) as shown in Fig. 2. It is not a true bipolar configuration due to the disc and outer ring being shorted. Lu and Tarjan[10] as well as Besio *et al.*[1] proposed this method to estimate the Laplacian potentials. Laplacian potentials can then be calculated as (6)

$$\Delta p_0 = \frac{(v_{\text{or}} + v_0)}{2} - v_{\text{mr}} \quad (6)$$

where v_{or} is the voltage on the outer ring,v_{mr} is the voltage on the middle ring, and v_0 is the voltage on the disc.

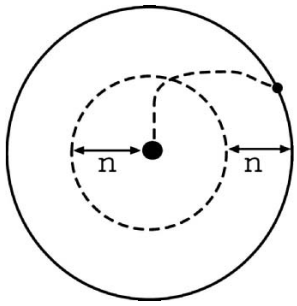

FIGURE 2. The concentric ring electrode can be configured as a bipolar (by neglecting the middle ring), quasi-bipolar electrode (by considering the short), or tri-polar (using all elements and neglecting the short). The interelectrode distance is *n*.

Nine-Point Method (NPM)

In Fig. 1, points p_1 to p_8 and p_0 form the nine-point arrangement. The Laplacian[7] of the potential at point p_0 as a result of the potentials v_1 through v_8 and v_0 at these respective points is given by

$$\left(\frac{\partial^2 v}{\partial x^2}+\frac{\partial^2 v}{\partial y^2}\right)\Bigg|_{p_0} = \Delta p_0 = \frac{1}{12r^2}\left\{16\sum_{i=1}^{4} v_i - 60v_0 - \sum_{i=5}^{8} v_i\right\} + O(r^4) \tag{7}$$

where $O(r^4) = \frac{r^4}{270}\left(\frac{\partial^6 v}{\partial x^6}+\frac{\partial^6 v}{\partial y^6}\right)\Big|_{P_0} + \cdots$, is the truncation error.

By comparing (1), (4), and (7) it can be observed that the NPM truncation error does not have the 4th order derivative term. Therefore, the NPM is considered to be more accurate than the FPM and QBM for approximating the Laplacian.

Applying the NPM to a Tri-Polar Electrode

The NPM is used as an approximation to a tri-polar concentric ring electrode. The following procedure is used to analyze a tri-polar electrode configuration as shown in Fig. 2, (three independent electrode elements). The nine-point arrangement can be seen as two FPMs. Points p_1, p_2, p_3, p_4, and p_0 form one FPM with a spacing of r, and points p_5, p_6, p_7, p_8, and p_0 form a second FPM with spacing of $2r$. By the same analysis used for the FPM, the NPM results in (A.6) and (A.8) as shown in the Appendix. Combining Equations (A.6) and (A.8) as $\{16\times(\text{A.6}) - (\text{A.8})\}$ cancels the fourth order term. Then the approximate solution for the Laplacian at point p_0 is

$$\Delta v_0 \cong \frac{1}{3r^2}\left\{16\left(\frac{1}{2\pi}\int_0^{2\pi} v(r,\theta)d\theta - v_0\right) - \left(\frac{1}{2\pi}\int_0^{2\pi} v(2r,\theta)d\theta - v_0\right)\right\} \tag{8}$$

where $\frac{1}{2\pi}\int_0^{2\pi} v(r,\theta)\,d\theta$ and $\frac{1}{2\pi}\int_0^{2\pi} v(2r,\theta)\,d\theta$ represents the average potentials on the middle ring and outer ring, respectively.

METHODS

Computer Model—Discrete Methods

To compare the different discrete methods-FPM, QBM, and NPM, a computer model was developed with a 400 × 400 mesh with spacing of 1/400 on a plane above a dipole oriented towards the positive direction of the Z-axis as shown in Fig. 3. On each point of this mesh, the electric potentials generated by a unity dipole were calculated with the formula[3] for electric potential due to a dipole in a homogeneous medium of conductivity σ

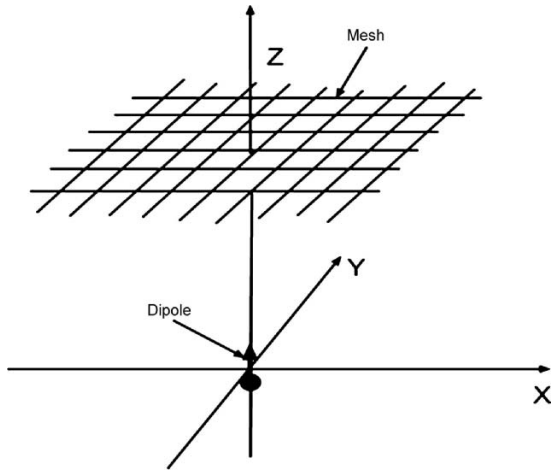

FIGURE 3. Schematic of the finite difference computer model, with a square mesh of size $N \times N$ and spacing $r = 1/N$, used for comparing the FPM, QBM, and NPM.

using (9)

$$\phi = \frac{1}{4\pi\sigma}\frac{(\bar{r}_p - \bar{r})\cdot\bar{P}}{|\bar{r}_p - \bar{r}|^3} \tag{9}$$

where $\bar{r} = (x, y, z)$ and $\bar{P} = (p_x, p_y, p_z)$ represent the location and moment of the dipole, and $\bar{r}_p = (x_p, y_p, z_p)$ represents the observation point. For this computer model it was assumed that $\bar{P}/4\pi\sigma$ was constant and the medium was homogeneous. The analytical Laplacian was then calculated at every point on the mesh, by taking the second derivative of the potential, i.e., (10).

$$L = \Delta\phi = \frac{\partial^2\phi}{\partial x^2} + \frac{\partial^2\phi}{\partial y^2} \tag{10}$$

According to He *et al*[3], this results in

$$L = \frac{3}{4\pi\sigma}\left[5(z_p - z)^2\frac{(\bar{r}_p - \bar{r})\cdot\bar{P}}{|\bar{r}_p - \bar{r}|^7} - \frac{(\bar{r}_p - \bar{r})\cdot\bar{P} + 2(z_p - z)p_z}{|\bar{r}_p - \bar{r}|^5}\right] \tag{11}$$

At each point on the mesh, the FPM, QBM, and NPM were applied to approximate the Laplacian with appropriate boundary conditions. This process was repeated for different interpoint distances using integer multiples of r. These estimates were then compared with the calculated analytical Laplacian for each point of the mesh by calculating the *Relative Error* and *Maximum Error*.[6]

$$\text{Relative Error}^i = \left[\frac{\sum(\Delta v - \Delta^i v)^2}{\sum(\Delta v)^2}\right]^{\frac{1}{2}} \tag{12}$$

$$\text{Maximum Error}^i = \max\left|\Delta v - \Delta^i v\right| \tag{13}$$

where i represents the method used to find the Laplacian and Δv represents the analytical Laplacian of the potential.

Computer Model—Continuous Methods

To compare the spatial filtering characteristics, the moving dipole computer model shown in Fig. 4 was considered. A unit dipole was moved in the X–Y plane and in the Z direction. The outer concentric ring electrodes ranged from 0.5 to 3.6 cm in diameter, with the middle ring sized proportionally from 0.25 to 1.8 cm in diameter. The modeled dipole was moved incrementally 0.5 cm at a time in the Z-axis from depths of 0.5 to 4.0 cm away from the tri-polar electrode. The dipole traversed the X-axis from –5.0 to 5.0 cm and in the Y-axis from –5.0 to 5.0 cm. The depth of the dipole was kept constant while it was moved in the X–Y plane along each preset path. The potentials on each electrode element were calculated using (9) for each incremental movement of the dipole in the X–Y plane. These potentials were then used to estimate the Laplacian for the three concentric ring electrode configurations: bipolar using (3), quasi-bipolar using (5), and the tri-polar using (8). Attenuation in dB of these estimated Laplacian potentials for the three configurations along the X direction were calculated and plotted.

To verify the spatial filter characteristics in the presence of noise, the above computer model was modified. A constant unity dipole representing the source of interest was modeled directly below the electrode and 20 noise source unit dipoles were placed at random locations. All the dipoles had the same orientation, directed towards the positive Z-axis. The constant dipole was always active and three to four of the noise dipoles were activated randomly. The Laplacian was calculated in the presence of the noise sources and the local sensitivity was verified for the three continuous electrode configurations.

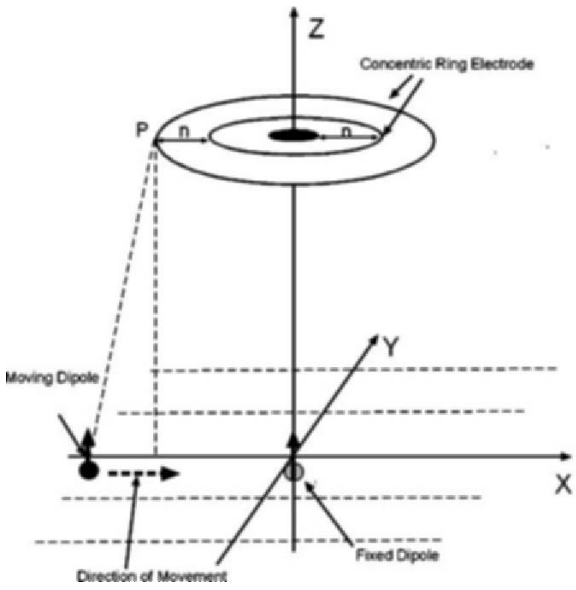

FIGURE 4. Schematic of the moving dipole computer model. The dipole was directed in the positive Z-axis and moved incrementally 1.0 cm at a time from –1.0 to –4.0 cm. The dipole was moved left to right from –5.0 to 5.0 cm along the X-axis. The middle ring was used for the quasi-bipolar and tri-polar electrode configurations.

Tank Experiments

Tank experiments were conducted in order to verify the results obtained by the closed form moving dipole computer model. A Plexi-Glass tank of size 50 × 26× 30 cm was filled with a saltwater mixture of 9 gm/l concentration, similar to that of human intracellular space. A dipole was constructed with two thin 1 mm radius copper discs, which were identically etched on both sides of a printed circuit board (PCB). Two 5 V pk–pk, 100 Hz AC square waves were then applied between the discs. The two discs were given alternating polarity square waves in order to limit the corrosion of the dipole discs.

The concentric electrodes were designed with ORCAD (Cadence) software and prepared using an LPKF ProtoMat® C20 rapid prototype board plotter (LPKF Laser & Electronics). The concentric electrodes were attached to a lead screw driven stage (T2312-A.5, Bell Screws & Actuators Co.) and moved along the X-axis on the surface of the saltwater at the rate of 1.8 cm/s. The experiment was repeated 20 times with a constant dipole depth and the data were averaged to minimize variations due to the experimental setup. Then the depth was changed and the measurements were repeated until all depths, 0.5, 1.0, 1.5, 2.0, 2.5, 3.0, 3.5, and 4.0 cm were completed. The potentials from the electrode elements in the tank experiments were compared with the closed form moving dipole computer model, using two concentric ring electrodes with outer ring diameters of 3.6 and 2 cm for the bipolar, quasi-bipolar and tri-polar configurations and 1.0 cm dipole depth. The disc had a diameter of 0.04 cm. The widths of the outer and middle rings were both set at 0.04 cm.

Potential measurements were taken from the three elements of the concentric ring electrodes using a custom LabView® (National Instruments) program via a National Instruments™ DaqCard 700. The measurements were referenced to an exposed electrode between the dipole discs. Post processing was achieved with a custom Matlab® (Mathworks) program. Laplacian potentials were calculated for bipolar, quasi-bipolar and tri-polar electrode configurations, using (3), (5), and (8), respectively. The attenuation in dB of the signals due to the distance along the radial axis was calculated and plotted for comparison between the three electrode configurations. The attenuation serves as a measure of the local sensitivity[11] and global noise rejection abilities of the three electrode configurations.

Tri-Polar Concentric Ring Electrode Active Sensor Design

An active sensor was designed for the tri-polar concentric ring electrode based on (8). According to (8), three differences have to be performed for the Laplacian potential: first, sixteen times the difference of the middle ring and center disc potential (let us assume this difference as A), second, the difference of the outer ring and center disc potentials (let us assume it as B), and third, the difference of these two differences (A–B).

An analog circuit was designed that performed these three differences with a band pass of 495 Hz (5 Hz low cutoff to 500 Hz high cutoff) and gain of 1000. The circuit was simulated using ORCAD PSpice®. This design was realized on two one-centimeter, two-layer PCBs using ORCAD. One of the PCBs had the tri-polar concentric ring electrode pattern, formed by two conducting rings and a conducting disc on the bottom side and signal processing circuitry on the opposite side as shown in Fig. 5(a). The other PCB had signal-conditioning circuitry on both layers of the board as shown in Fig. 5(b).

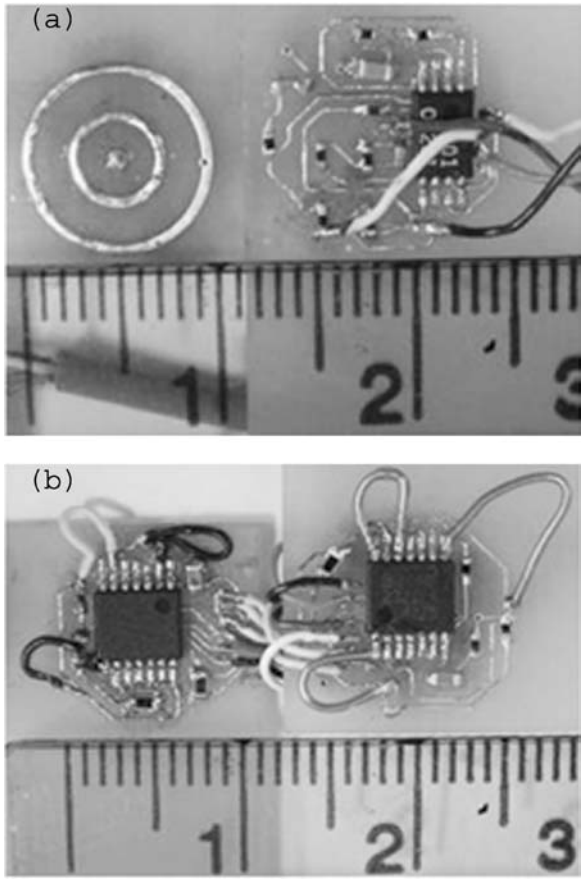

FIGURE 5. The one-centimeter active Laplacian tri-polar sensor: (a) top and bottom layers of the first board, (b) top and bottom layers of the second board.

ECG signals were recorded from two healthy human subjects in accordance with the IRB approved protocol using the one-centimeter active Laplacian tri-polar sensor. Signals were acquired to a laptop computer using a DATAQ® DI-720 data acquisition system during 30-s recordings, at a sampling rate of 1000 samples per second. These signals were filtered digitally using a custom Matlab® program to remove 60 Hz power line noise and ensemble averaged to attenuate other random noise and finally LECG signals were plotted.

Statistics

One-way analysis of variance (ANOVA) with post hoc *t*-test and Bonferroni corrections was performed to compare: (1) Relative and Maximum Errors between the FPM, QBM, and NPM, (2) the attenuation between the bipolar, quasi-bipolar, and tri-polar configurations in the moving dipole model, and (3) the attenuation between the bipolar, quasi-bipolar, and tri-polar configurations in the tank experiments.

RESULTS

Error Comparison Between the FPM, QBM, and NPM Using Discrete Method Computer Models

Relative and Maximum errors of the FPM, QBM, and NPM were calculated using formulae (12) and (13). The errors were plotted for different inter point distance (i.e. integer multiples of r) on a semi-log graph as shown in Fig. 6. The Relative and Maximum Errors were significantly smaller for the NPM than the FPM and QBM ($p < 0.0001$, one-way ANOVA).

Comparison of Bipolar, Quasi-Bipolar and Tri-Polar Configurations Using Moving Dipole Computer Model and Tank Experiments

Laplacian potentials were calculated for the three electrode configurations using the moving dipole computer model shown in Fig. 4. These values were calculated as the dipole moved along the X-axis from -5 to 5 cm at $Y = 0$. As the dipole moved away from the origin, dB attenuation of the Laplacian potentials for the three electrode configurations was calculated for a dipole depth of 1.0 cm, a 2.0 cm diameter electrode, and plotted as shown in Fig. 7 panel A. The tri-polar configuration had greater attenuation than the bipolar and quasi-bipolar configurations ($p < 0.0001$, one-way ANOVA). A single path along the X-axis was taken instead of different parallel paths as shown in Fig. 4. This simplification could be made since the attenuation in all directions was equal due to symmetry. From Fig. 7 panel A, the radial distance for an attenuation of 20 dB can be compared as a measure of local sensitivity: bipolar electrode 0.65 cm, quasi-bipolar electrode 0.9 cm and tri-polar electrode 0.55 cm. The radial distance is a measure of the electrodes sensitivity to sources, the

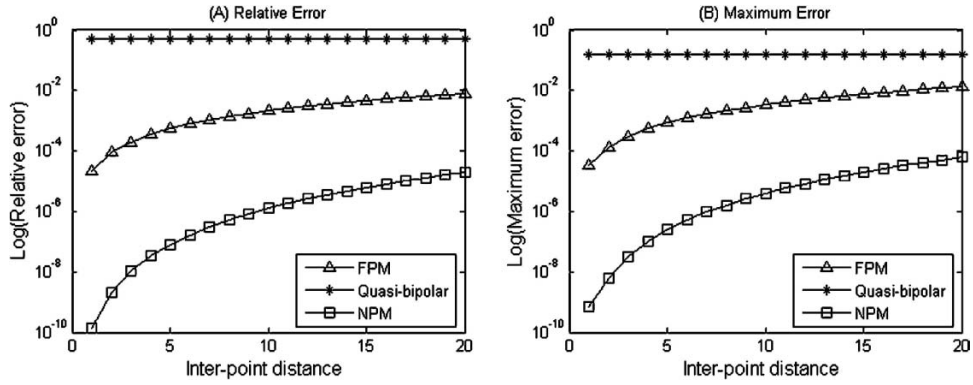

FIGURE 6. (A) Relative Error and (B) Maximum Error of the FPM, QBM, and NPM in estimating the Laplacian when compared to the analytical Laplacian. Logarithmic scale was used on the Y-axis.

shorter the distance, the more sensitive the electrode is. As shown in Fig. 7 panel B, the tri-polar configuration still had greater attenuation than the bipolar and quasi-bipolar configurations even when random dipoles simulating noise were introduced at a depth of 1.0 cm in addition to the dipole signal source. This shows that the tri-polar electrode possesses better local sensitivity and is more sensitive to local sources than the other configurations analyzed. This local sensitivity was verified again in the tank experiments. The results from the tank experiments also showed that the tri-polar electrode configuration had significantly greater attenuation than the bipolar and quasi-bipolar electrode configurations ($p < 0.0001$, one-way ANOVA).

Validation of Moving Dipole Computer Model with Tank Experiments

The attenuation in dB of the Laplacian potentials of the three electrode configurations was calculated from the tank experiment data for two electrode sizes. The outer concentric ring electrode diameters were 2.0 and 3.6 cm, respectively. A dipole at a depth of 1 cm was held stationary while the electrode moved from −5.0 to 5.0 cm along the X-axis with $Y = 0$. Experimentally measured attenuations in dB for the three configurations were compared with the simulated data. The plots of the attenuation for the bipolar (A), quasi-bipolar (B), and tri-polar (C) configurations are shown for a 2.0 cm diameter electrode in Fig. 8 and for a 3.6 cm diameter electrode in Fig. 9. The cross-correlation was calculated between the attenuation data of the closed-form moving dipole computer model and tank experiment data. The cross-correlation coefficient was 0.87 ± 0.05. In both Figs. 8 and 9 it can be seen that at a radial distance of 1.0 cm the attenuation is the greatest for the tri-polar electrode configuration at –93 and –98 dB, respectively. It can also be observed that at 4.0 cm the attenuation is the greatest for the tri-polar electrode configuration at approximately—124 dB.

Human LECG Recordings

Once all of the computer models and tank experiments showed that the tri-polar electrode configuration had advantages over the bipolar and quasi-bipolar electrode configurations, it was time to verify that tri-polar LECG could really be recorded from humans. The active sensors were designed, assembled, and verified for gain and band pass. To record from humans, the subjects were first seated in a comfortable chair. Then a one-centimeter diameter active Laplacian tri-polar sensor was placed on their chests at the intersection of the mid-sternal and nipple lines. Two-

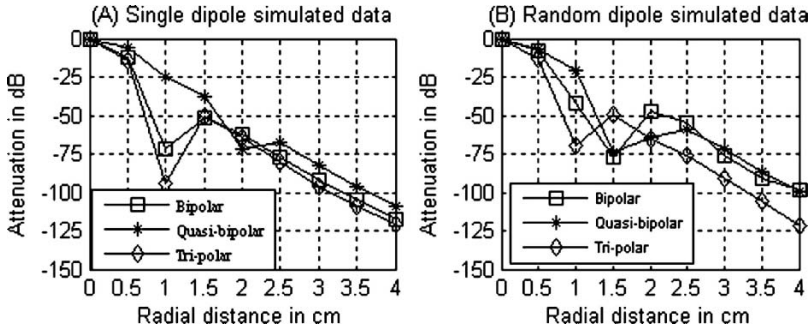

FIGURE 7. (A) Simulated data of attenuation in dB for the three configurations as the dipole departs from the origin along the X-axis, (B) same as (A) with the addition of noise due to random dipoles.

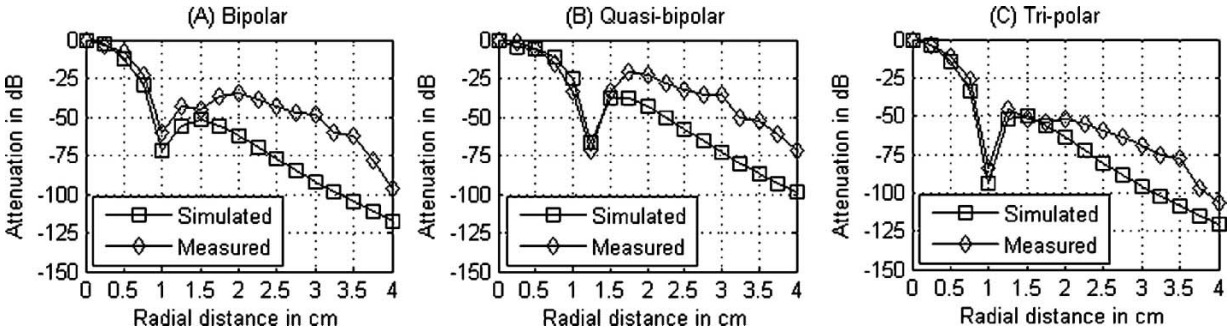

FIGURE 8. Comparison of measured attenuation in dB with the simulated attenuation in dB of Laplacian potentials for a concentric ring electrode of 2.0 cm outer diameter and dipole depth of 1.0 cm: (A) bipolar configuration, (B) quasi-bipolar configuration, and (C) tri-polar configuration.

channels of data, LECG and Lead II ECG, were recorded and processed further as mentioned in the Methods. Fig. 10(A) shows the LECG recorded and processed from one of the healthy human subjects. Fig. 10(B) shows the Lead II ECG recorded concurrently from the same subject.

DISCUSSION

The FPM and QBM have truncation errors of the order r^2 whereas the NPM has the order of r^4. Hence, it is expected that the NPM would be more accurate than the FPM and QBM in estimating the Laplacian, which is proven by the analysis of the computer models developed for this paper. The statistical analysis comparing Maximum and Relative Errors between the FPM, QBM, and NPM showed that the NPM had significantly less error in approximating the Laplacian.

From analysis of the measured tank experiment data and the simulated data of the 2.0 cm diameter concentric ring electrode, it was determined that the tri-polar electrode had greater local sensitivity[9] than the bipolar and quasi-bipolar electrode configurations. As noted in the Results section, the width of the signal at the 20 dB points in Fig. 7(A) is less for the tri-polar electrode than the others: 0.55 (tri-polar) vs. 0.65 cm (bipolar) and 0.9 cm (quasi-bipolar). What this means is that the tri-polar electrode has a narrower radial distance for accepting signals than the bipolar and quasi-bipolar electrodes. This increased local sensitivity enhances localization of sources. As illustrated in Figs. 7(A) and 7(B), without/with noise sources, the tri-polar trace exhibits the greatest attenuation for off center sources. This finding is very beneficial for discrimination of global sources such as noise. For instance, while recording the electrical activity of the heart, the subject may be moving which generates electromyograms that can distort the ECG signal. With the tri-polar electrode such global noise signals are attenuated more than with the bipolar and quasi-bipolar electrodes.

An evaluation of the attenuation traces in Fig. 8 for the 2.0 cm and Fig. 9 for the 3.6 cm diameter electrode configurations highlights that the shapes of the attenuation of off center sources for the three configurations in the computer modeled data are very similar as compared to the measured data from the tank experiments (with cross-correlation coefficient of 0.87 $\pm$ 0.05). Since a unity dipole was used as the source of the computer model, it is not possible to achieve a direct magnitude comparison between the computer model and the tank experiments. The use of a more realistic dipole source could help enhance these findings. Another area of our analysis that can be improved is to use multiconductivity models, both for computer modeling and

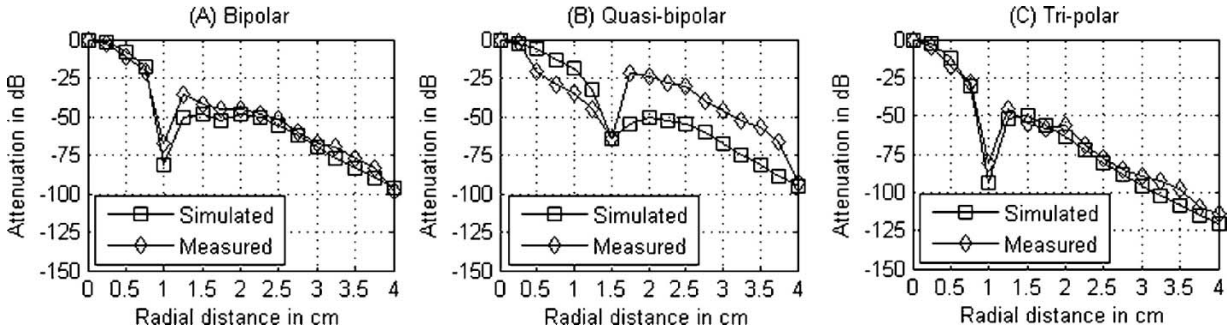

FIGURE 9. Comparison of measured attenuation in dB with the simulated attenuation in dB of Laplacian potentials for a concentric ring electrode of 3.6 cm outer diameter and dipole depth of 1.0 cm: (A) bipolar configuration, (B) quasi-bipolar configuration, and (C) tri-polar configuration.

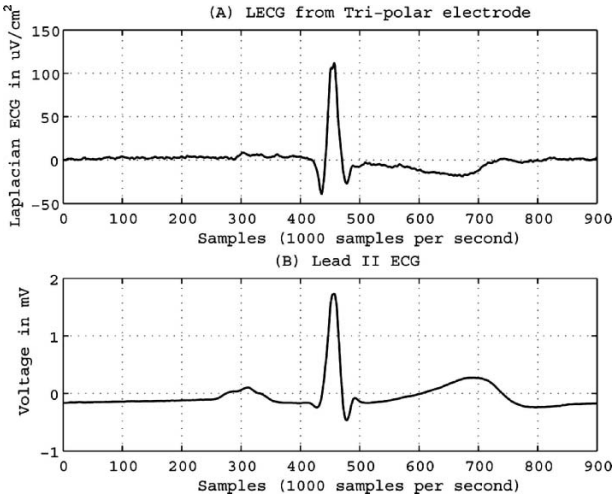

FIGURE 10. Digitally filtered signal recorded from a healthy human subject: (A) when the one-centimeter diameter active sensor was placed at the intersection of the midsternal and nipple lines, (B) Lead II ECG signal.

physical verification experiments. The different conductivities will alter the potentials calculated and measured; the potentials will decrease as conductivities are lowered. Even with the reduced potentials, we should still achieve the same outcome that the tri-polar concentric ring electrode configuration was significantly better for accuracy and attenuation than the bipolar or quasi-bipolar concentric ring electrode configurations since the reduction of potentials should be relative to each configuration.

There are still other possible reasons for the difference between the simulated and measured values. This difference can be justified by a scaling factor, which originates from negligence in the computer model of conductivity for saltwater and permittivity of the printed circuit board material between the two thin discs of copper used to construct the dipole. The tank experiments disclosed that there are also ambient noise sources and nonideal alignments of electrodes and dipoles that alter signals from the ideal conditions of the computer model. One final point about the difference between the computer models and the tank experiments can be found in negligence of the multielement electrode interactions in the computer model. The potentials on each element of the electrodes interact with each other altering the potentials slightly. For larger potentials there would be greater interaction. In the tank experiments we are using sources with a potential difference of 10 V. Body surface Laplacian potentials are typically a few hundred microvolts, which should not cause significant interference. More accurate computer models and higher precision mechanisms for positioning the dipoles and concentric electrodes in the tank experiments can remedy these shortcomings.

The magnitude of the dipole in the tank experiments was set to 10 Vpp, which is unrealistic. Setting the dipole potential high allowed us to acquire the data from the concentric electrodes without the use of amplifiers. Actual magnitudes of Laplacian body surface potentials would be different from those of the tank experiments or computer models. The shape of the signals due to radial distance was the critical information obtained from these experiments. The attenuation due to radial distance showed that the tri-polar electrode design had the most local sensitivity. The final proof of concept is in the acquisition of real cardiac signals, which is discussed next.

Based on the tri-polar configuration, which was shown to be an extension of the NPM, a one-centimeter diameter active Laplacian tri-polar sensor was developed and cardiac signals were recorded successfully from humans. The active sensor was realized with surface mount SOIC components on two stacked printed circuit boards. A 1 cm diameter was chosen for a 2.0 mm spatial resolution. The gaps between the electrodes were initially set to 1.0 mm; however, the signal clarity was not appropriate at this spatial resolution. As shown by the signals presented in Fig. 10, the 2.0 mm gap spacing works well for acquiring Laplacian ECG. With better instrumentation, it may be possible to realize a sensor with less than 2.0 mm gap spacing to increase the spatial resolution.

The LECG signals were acquired at various locations over the thorax surface of the subjects, even from the back. Only the LECG signal acquired at the intersection of the mid-sternal and nipple lines is shown in Fig. 10. The LECG, even though recorded with an interelectrode spacing of only 2.0 mm, still has a clear signal. A close analysis of the two traces of Fig. 10 reveals that the LECG has slightly steeper slopes during the R-wave. The base of the Lead II ECG trace is 32 ms wide while the LECG base is only 26 ms wide due to the sharper local sensitivity of the second spatial derivative.

CONCLUSIONS

The tri-polar configuration/NPM results in significantly more accurate approximation to the analytical Laplacian than the bipolar configuration/FPM and quasi-bipolar configuration/QBM. The tri-polar configuration is also significantly superior for attenuating global sources than the bipolar and quasi-bipolar configurations. This property increases the local sensitivity and will be beneficial in localizing sources and rejecting global signals such as artifact due to muscle activity from limb movement while recording cardiac signals. By detecting differences on the concentric electrode elements, it is possible to measure the potentials due to localized cardiac activity with extremely high attenuation of global sources that would be considered noise. The 1 cm diameter active Laplacian tri-polar sensor performed as designed and has been shown to be feasible for acquiring LECG signals on the thoracic surface of humans. With a dense array of these active sensors, it will

be possible to record high spatial and temporal resolution LECG.

Further work is necessary to evaluate artifact rejection and develop an LECG mapping system. A more complex model with realistic source magnitudes would be more accurate in predicting potentials measured with the electrodes. It would be more accurate to include multiconductive layers for the different thoracic compartments as well as skin and muscles. We are presently developing an integrated model to accomplish this task.

APPENDIX

Since the proposed quasi-bipolar electrode shown in Fig. 2 has equal interelectrode distance, the analysis of the nine-point arrangement formed by points p_1 through p_8 and p_0 of Fig. 1, with the same interpoint distance, is considered. Voltages v_0 through v_8 are the potentials at these points. Each potential in this nine-point arrangement can be written in the form of a Taylor series expansion as explained by Huiskamp.[6]

The average of the outer potentials v_5, v_6, v_7, and v_8 after the Taylor series expansion becomes

$$\frac{v_5+v_6+v_7+v_8}{4} = v_0 + r^2\left(\frac{\partial^2 v}{\partial x^2}+\frac{\partial^2 v}{\partial y^2}\right)\Bigg|_{p_0} + \frac{r^4}{3}\left(\frac{\partial^4 v}{\partial x^4}+\frac{\partial^4 v}{\partial y^4}\right)\Bigg|_{p_0}+\cdots \tag{A.1}$$

The average of the potentials v_1, v_2, v_3, and v_4 after the Taylor series expansion becomes

$$\frac{v_1+v_2+v_3+v_4}{4} = v_0 + \frac{r^2}{4}\left(\frac{\partial^2 v}{\partial x^2}+\frac{\partial^2 v}{\partial y^2}\right)\Bigg|_{p_0} + \frac{r^4}{48}\left(\frac{\partial^4 v}{\partial x^4}+\frac{\partial^4 v}{\partial y^4}\right)\Bigg|_{p_0}+\cdots \tag{A.2}$$

Adding v_0 to both sides of (A.1) and then dividing by 2 gives

$$\frac{\frac{1}{4}\sum_{i=5}^{8} v_i + v_0}{2} = v_0 + \frac{r^2}{2}\left(\frac{\partial^2 v}{\partial x^2}+\frac{\partial^2 v}{\partial y^2}\right)\Bigg|_{p_0} + \frac{r^4}{6}\left(\frac{\partial^4 v}{\partial x^4}+\frac{\partial^4 v}{\partial y^4}\right)\Bigg|_{p_0}+\cdots \tag{A.3}$$

Subtracting (A.2) from (A.3) results in

$$\frac{1}{2}\left(\frac{1}{4}\sum_{i=5}^{8} v_i + v_0\right) - \frac{1}{4}\sum_{j=1}^{4} v_j = \frac{r^2}{4}\left(\frac{\partial^2 v}{\partial x^2}+\frac{\partial^2 v}{\partial y^2}\right)\Bigg|_{P0} + \frac{7r^4}{48}\left(\frac{\partial^4 v}{\partial x^4}+\frac{\partial^4 v}{\partial y^4}\right)\Bigg|_{p_0}+\cdots \tag{A.4}$$

From (A.4) the approximate solution for the Laplacian of the potential at p_0 can be estimated. Therefore, the Laplacian at p_0 is

$$\Delta p_0 = \left(\frac{\partial^2 v}{\partial x^2}+\frac{\partial^2 v}{\partial y^2}\right)\Bigg|_{p_0} = \frac{4}{r^2}\left[\frac{1}{2}\left(\frac{1}{4}\sum_{i=5}^{8} v_i + v_0\right) - \frac{1}{4}\sum_{j=1}^{4} v_j\right] + O(r^2)\ldots \tag{A.5}$$

where $O(r^2) = \frac{2}{r^2}[O(r^4)] = \frac{7r^2}{48}\left(\frac{\partial^4 v}{\partial x^4}+\frac{\partial^4 v}{\partial v^4}\right)\Big|_{p_0}+\cdots$ is the truncation error.

Equation (A.5) can also be generalized to the quasi-bipolar concentric ring electrodes, neglecting the truncation error $O(r^2)$. By applying a similar procedure as was used for the bipolar electrode configuration, performing the integral along a circle of radius r around point p_0 of the Taylor expansion and defining $X = r\sin(\theta)$ and $Y = r\cos(\theta)$ [6] result in (A.6), which is the potential on the middle ring.

$$\int_0^{2\pi} (v(r,\theta)d\theta = \int_0^{2\pi} v_0\, d\theta + \frac{r^2}{4}2\pi\Delta v_0 + \frac{r^4}{24}\int_0^{2\pi}\sum_{j=0}^{4}(\sin\theta)^{4-j}(\cos\theta)^j d\theta\left(\frac{\partial^4 v}{\partial x^{4-j}\partial y^j}\right)\Bigg|_{p_0} + \frac{(2r)^6}{6!}\int_0^{2\pi}\sum_{j=0}^{6}(\sin\theta)^{6-j}(\cos\theta)^j\theta\left(\frac{\partial^6 v}{\partial x^{6-j}\partial y^j}\right)\Bigg|_{p_0} + \cdots\cdots \tag{A.6}$$

Similarly performing the integral along a circle of radius $2r$ around p_0 and defining $X = 2r\sin(\theta)$ and $Y = 2r\cos(\theta)$[6] result in (A.7), which is the potential on the outer ring.

$$\int_0^{2\pi} v(2r,\theta)d\theta = \int_0^{2\pi} v_0 d\theta + r^2 2\pi\Delta v_0 + \frac{2r^4}{3}\int_0^{2\pi}\sum_{j=0}^{4}(\sin\theta)^{4-j}(\cos\theta)^j d\theta\left(\frac{\partial^4 v}{\partial x^{4-j}\partial y^j}\right)\Bigg|_{p_0} + \frac{(2r)^6}{6!}\int_0^{2\pi}\sum_{j=0}^{6}(\sin\theta)^{6-j}(\cos\theta)^j d\theta\left(\frac{\partial^6 v}{\partial x^{6-j}\partial y^j}\right)\Bigg|_{p_0} + \cdots \tag{A.7}$$

Adding the potential of the disc, $\int_0^{2\pi} v_0\, d\theta$, to both sides of (A.7) and then dividing by 2 results in the average of outer ring and center disc potentials, representing the short

in the quasi-bipolar method. This results in

$$\frac{\int_0^{2\pi}(v(2r,\theta)+v_0)d\theta}{2} = \int_0^{2\pi} v_0\,d\theta + r^2\pi\,\Delta v_0 + \frac{r^4}{3}\int_0^{2\pi}\sum_{j=0}^{4}(\sin\theta)^{4-j}(\cos\theta)^j d\theta\left(\frac{\partial^4 v}{\partial x^{4-j}\partial y^j}\right)\Bigg|_{p_0} + \cdots \quad \text{(A.8)}$$

Neglecting the truncation error and subtracting Equation (A.6) from (A.8) result in a proportionate approximation (A.9) to the Laplacian at point p_0 using the quasi-bipolar concentric ring electrode.

$$\Delta v_0 \cong \frac{4}{r^2}\left(\frac{\frac{1}{2\pi}\int_0^{2\pi}(v(2r,\theta)+v_0)d\theta}{2} - \frac{1}{2\pi}\int_0^{2\pi} v(r,\theta)d\theta\right) \quad \text{(A.9)}$$

where $\frac{1}{2\pi}\int_0^{2\pi} v(r,\theta)\,d\theta$ and $\frac{1}{2\pi}\int_0^{2\pi} v(2r,\theta)d\theta$ represent the average potentials on the middle ring and outer ring, respectively.

ACKNOWLEDGMENTS

The authors thank Louisiana Tech University Center for Entrepreneurship and Information Technology, Louisiana Board of Regents (grant # LEQSF (2003–05)-RD-B-05), and the NCIIA for financial support and our lab associates and Dr. Aijun Besio for their assistance in this research and manuscript.

REFERENCES

[1]Besio, W., C. C. Lu, and P. P. Tarjan. A feasibility study for body surface cardiac propagation maps of humans from Laplacian moments of activation. *Electromagnetics* 21:621–632, 2001.

[2]Fattorusso, V., and J. Tilmant. Exploration du champ electrique precordial a l'aide de deux electrodes circulaires, concentriques et rapprochees. *Arch. Mal du Coeur.* 42:452–455, 1949.

[3]He, B., and D. Wu. Laplacian electrocardiography. *Crit. Rev. BME* 27(3–5):285–338, 1999.

[4]He, B., and R. J. Cohen. Body surface Laplacian ECG mapping. *IEEE Trans. BME* 39(11):1179–1191, 1992.

[5]He, B., and R. J. Cohen. Body surface Laplacian mapping in man. *IEEE EMBS* 13(2):784–786, 1991.

[6]Huiskamp, G. Difference formulas for the surface Laplacian on a triangulated surface. *J. Comput. Phys.* 95(2):477–496, 1991.

[7]Lapidus, L., and G. F. Pinder. Numerical Solution of Partial Differential Equations in Science and Engineering. New York: John Wiley & Sons, Inc.,1982, 371–372.

[8]Lian, J., G. Li, J. Cheng, B. Avitall, and B. He. Body surface Laplacian mapping of atrial activation in normal subjects. *Med. Biol. Eng. Comput.* 40(6):650–659, 2002.

[9]Li, G., J. Lian, P. Salla, J. Cheng, P. Shaw, I. Ramachandra, B. Avitall, and B. He Body surface Laplacian mapping of ventricular depolarization in normal subjects. *J. Cardiovasc. Electrophysiol.* 14(1):16–27, 2003.

[10]Lu, C. C., and P. P. Tarjan. An ultra high common mode rejection ratio (CMRR) AC instrumentation amplifier for Laplacian electrocardiographic measurements. *Biomed. Instr. Tech.* 76–93, Jan–Feb, 1999.

[11]Oosterom, A. V., and J. Strackee. Computing the lead field of electrodes with axial symmetry. *Med. Biol. Eng. Comput.* 21:473–481, 1983.

[12]Ames, W. F. *Numerical Methods for Partial Differential Equations*. New York: Barnes & Noble, Inc. 1969, 15–19.